Tailored polymer microlenses on treated glass surfaces

Mordechai Sokuler
Department of Biotechnology Engineering, Ben-Gurion University of the Negev, P.O. Box 653, Beer-Sheva 84105, Israel

Daniel Aronov and Gil Rosenman
Department of Electrical Engineering—Physical Electronics, Tel Aviv University, Tel Aviv 69978, Israel

Levi A. Gheber[a)]
Department of Biotechnology Engineering, Ben-Gurion University of the Negev, P.O. Box 653, Beer-Sheva 84105, Israel

(Received 20 February 2007; accepted 27 April 2007; published online 16 May 2007)

Integrating arrayed biosensors (biochips) or micro- and nanofluidic devices with readout systems is an important step towards their realization in lab-on-a-chip devices. To this end, we present a straightforward method of fabricating polymer microlenses in precise locations, with desired optical characteristics, using a combination of two methods: surface energy tuning using low-energy electron irradiation, to control the numerical aperture, and time-controlled nanofountain pen deposition of polymer microlenses, to control the focal length. The authors demonstrate the tuning of focal length between 8 and 20 μm with numerical apertures between 0.16 and 0.26. © *2007 American Institute of Physics*. [DOI: 10.1063/1.2739087]

The continued miniaturization of biochips is expected to tremendously increase their portability, thus expanding the use of these arrayed biosensors to point-of-care clinical testing, environmental monitoring, etc. Indeed, constant advances towards nanobiochips are being reported (see, for example, Refs. 1 and 2). However, the expected decrease in fluorescence signal, due to reduction in the number of biological molecules as well as the need to integrate the optical reading systems with the biochip suggest that small optical elements, strategically positioned and with tailored optical characteristics, should help to overcome some of the expected challenges.

We have previously demonstrated the manufacture of polymer microlenses using nanofountain pen (NFP) to achieve precise positioning of single lenses in locations of interest and to enhance the fluorescent light emitted by model nanobiochip spots.[3] Using NFP, we deposited droplets of monomer solution and subsequently polymerized them to yield microlenses. There we were able to control the focal length of those lenses, by varying the deposition time, an approach that while elegant (a single experimental parameter) is limited to constant numerical aperture (NA) lenses (determined by the contact angle the drops make with the surface).

To change independently the lens NA, one needs to controllably change the angle of contact between the monomer solution and the surface, which is determined, among others parameters, by the surface energy of the substrate. Diverse techniques of surface energy modification have been developed, such as deposition of self-assembled monolayers (SAMs), electrical, light-induced, and electrochemical methods.[4,5] Among these methods, the formation of SAMs proved to be a simple and practical technique for controlling wettability.[4] However, the aforementioned techniques are either accompanied by surface chemical reactions or phase transitions and creation of defects which may interfere with the other functions of a biochip. In addition, it is difficult to achieve homogenous wetting properties over large surfaces, and gradual variation of wettability is not possible, with these techniques.

Here we utilize an alternative approach to gradual tuning of the wettability of glass surfaces, induced by low electron energy irradiation.[6,7] Electron/hole charges, generated by the electron beam, are trapped in the vicinity of the glass substrate surface. Such a treatment results in significant wettability tuning. This method allows fabricating either homogenous distribution or patterning of the wettability states with high resolution. This effect[6] was also demonstrated in other solid state materials, such as amorphous silicon dioxide, silicon nitride, mica, alumina, *n*- and *p*-silicon, metals (aluminium and titanium, which are always coated with thin oxide films), and biomimetic materials (hydroxyapatite, sea shells, etc.).[8]

Specimens of 10 mm square were cut from a standard microscope glass slides for surface treatment. Prior to electron-beam exposure, the glass specimens were cleaned by sonicating in isopropanol (95%, Sigma) for 2 min. and rinsed with de-ionized water. Electron irradiation was performed in high vacuum (10^{-6} Torr) at room temperature, using a Kimball Physics electron gun with constant electron energy of 120 eV and current density of 100 nA cm^{-2}. The exposure time was varied from 0 to 20 min, with a corresponding maximum incident charge density of 120 μC cm^{-2}. Based on a Monte-Carlo simulation method, we estimate a penetration depth of the incident electrons of approximately 3 nm, consistent with the analytical solution.[9]

Cantilevered nanopipettes (600 nm aperture diameter, Cr/Au covered cantilevers of 500–600 μm length, Nanonics Ltd., Jerusalem, Israel) were filled with a mixture of 2,2-dimethoxy-2-phenylacetophenone (Fluka) and trimethylolpropane trimethacrylate (Sigma), in a ratio of 1 mg:1 ml. The pipettes, mounted as the probe of an atomic force microscope (AFM), were used to deliver the fluid to irradiated surfaces, where it formed lens-shaped drops. Once a set of droplets was deposited on a surface, they were polymerized in argon atmosphere under 6 W irradiation of wavelength of

[a)]Electronic mail: glevi@bgu.ac.il

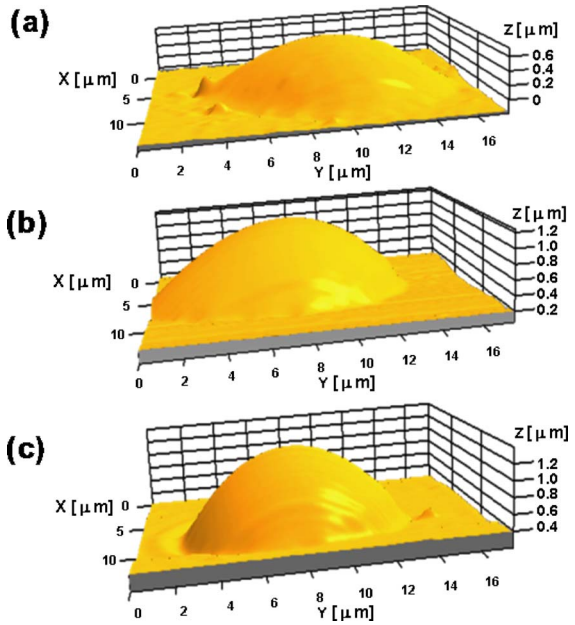

FIG. 1. (Color online) 3D rendering of AFM scans of three lenses, all fabricated with a 600 nm diameter pipette, using the same deposition time (10 s) and the same prepolymerization fluid. (a) A surface charge density of 120 μC cm^{-2} led to a contact angle α=11°. (b) The measured contact angle here is α=16°, with a treatment resulting in 50 μC cm^{-2} surface charge density. (c) The measured contact angle of this lens is α=22° on a surface irradiated with a surface charge density of 5 μC cm^{-2}.

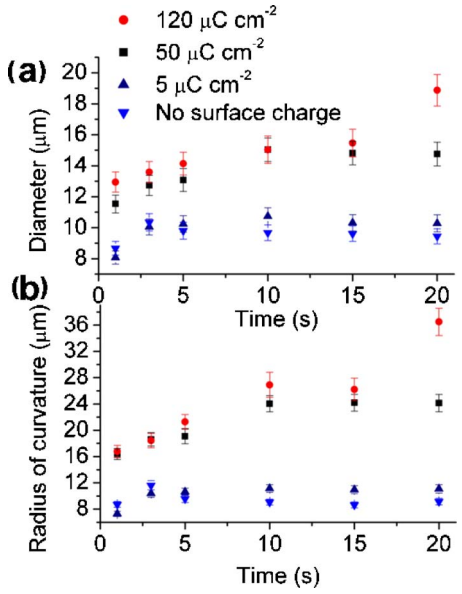

FIG. 2. (Color online) Diameters of lenses ranging between 8 μm (untreated surface) and 19 μm (sample with surface charge density of 120 μC cm^{-2}) for deposition time ranging between 1 and 20 s, respectively. It can be seen that the treated surfaces produce differing geometric properties of the lenses having kept all other parameters nominally constant. (a) The lens'diameters increased with rise in surface charge density. (b) The radius of curvature of the lenses increased with higher surface charge density.

254 nm from a Vilber Lourmat UV lamp, at a distance of 3 cm from the light source, for 5 min. AFM characterization of the microlenses was performed using "ultrasharp" gold-covered silicon contact cantilevers (Mikromasch, CSC12/CR-Au/15) in contact mode. Resulting microlenses were characterized using a Zeiss Axioplan2 microscope with a 20×, 0.5 NA objective and a SPOT (Diagnostic Instruments inc.) digital camera.

Glass slides were electron treated to produce three types of surfaces with 5, 50, and 120 μC cm^{-2} surface charge densities respectively. The same pipettes were used to deposit drops on all surfaces by contacting the *m* with each surface for various durations between 1 and 20. The resulting lenses were investigated with AFM and bright-field microscopy to characterize their geometry and optical properties, respectively.

AFM scans of the polymerized droplets reveal that they form smooth spherical caps, with an rms roughness of ~1.6 nm (not shown). The qualitative influence of the surface treatment is demonstrated in FIG. 1, which shows a three-dimensional (3D) representation of three microlenses, all with the same deposition time (10 s), manufactured on differently treated surfaces. It is readily visible that the lenses have a larger diameter and radius of curvature, and a decreasing contact angle, with increasing electron irradiation dose of the surface.

The quantitative effects of change in surface energy are shown in Fig. 2, which presents a summary of all the sets of lenses written on the three treated surfaces and one (untreated) control surface. The dependence of the lens diameter on deposition time for each surface is plotted in Fig. 2(a), and for each surface the lens diameter increases with deposition time in a nonlinear fashion, approaching an asymptotic value for long deposition times. For the same deposition time, increasing diameters are obtained for surfaces with higher surface charge density. Figure 2(b) shows a plot of the AFM measured radius of curvature *R* of the lenses as a function of the deposition time. For a given surface, the contact angle is constant, giving rise to a linear dependence of *R* on the diameter *D* of the form

$$R = \frac{D}{2 \sin \alpha}, \tag{1}$$

where α is the contact angle. This explains the qualitatively similar behavior of the plots describing the diameter and radius of curvature (Figs. 2(a) and 2(b), respectively). Importantly, the radius of curvature depends on the diameter and thus, on the deposition time and also on the contact angle, which is changed by the irradiation of the surfaces. Using both parameters leads to the ability to modulate the radius of curvature by as much as 30 μm (from 8 to 38 μm).

Placing the lenses on the stage of a microscope, a collimated beam of white light was projected on them by positioning the condenser appropriately. Sets of images of the lenses were taken at varying *Z* planes, 2.5 μm apart, through the focal plane. Figure 3(a) depicts such a set of images taken through a microlens manufactured with 15 s deposition time, on a surface with 50 μC cm^{-2} surface charge density. For each microlens, such images were then stacked in the *Z* direction, and sectioned in the *Z-X* plane, to obtain intensity distribution maps. Figure 3(d) shows such maps for lenses manufactured with 15 s deposition time on three surfaces treated with different doses of electron irradiation (5, 50, and 120 μC cm^{-2}, as indicated). The intensity along the *Z* (optical) axis was extracted, fitted with a Gaussian curve and the peak was taken to represent the focal length of the particular lens. Figure 3(c) shows three such plots corresponding to the lenses described in Fig. 3(d). Once the focal plane was determined, an intensity profile in the focal plane along the *X* (or *Y*) direction was extracted. The width of the Gaussian

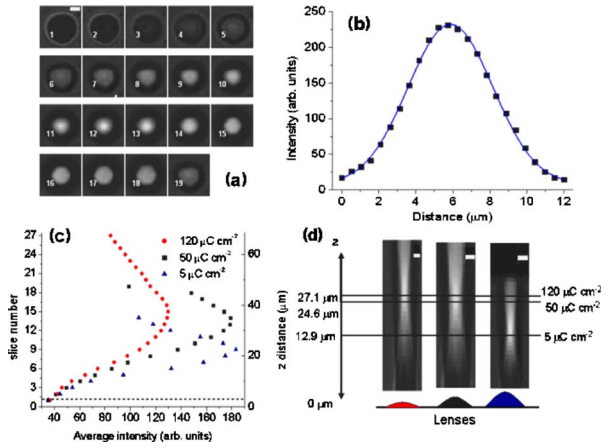

FIG. 3. (Color online) Optical characterization of microlenses. (a) A series of images of light focused through one micro lens (15 s deposition time, on a surface with 50 μC cm^{-2} surface charge density), starting below the plane of the lens (slice 1) through the focal plane (slices 11–13) and above it (slices 14–18). White scale bar in slice 1 represents 8 μm. (b) The intensity profile along the X or Y axis of the lens in (a) taken at the focal plane, with a full width at $1/\sqrt{e}$ of 5.7 μm. (c) The intensity profiles along the Z axis (optical axis of the lenses) for 15 s deposition time lenses on surfaces with different charge densities of 5, 50, and 120 μC cm^{-2}, as indicated. The dashed horizontal line represents the plane of the lenses. The focal length (the position of the curve peak) and the depth of field (the width of the curve) differ for each lens. (d) Stacks formed of slices as in (a) were sectioned along the X-Z plane, to obtain the light intensity distribution in this plane, for the all the treated surfaces. White scale bars are representative of 8 μm. The solid lines indicate the focal planes of the lenses, numbers to the right give the surface charge densities, and the numbers on the left give the focal lengths.

fitted to such profiles represents the diffraction limited focal spot of the lenses. Figure 3(b) shows such a profile for the lens described in Fig. 3(a).

Since the focal length of a lens is determined by its radius of curvature according to

$$f = \frac{R}{n_{\text{lens}} - 1}, \tag{2}$$

or, substituting R from Eq. (1),

$$f = \frac{D}{2(n_{\text{lens}} - 1)\sin\alpha}, \tag{3}$$

the focal length can be tuned by using any combination of deposition time [which determines D, see Fig. 2(a)] and surface electron irradiation (which determines α). On the other hand, the numerical aperture only depends on the contact angle α, thus on a surface with a given irradiation dose, the contact angle is fixed and so is the NA [with the use of Eq. (3)],

$$\text{NA} = \frac{nD}{2f} = 2n(n_{\text{lens}} - 1)\sin\alpha, \tag{4}$$

where n is the refractive index of the medium through which light is propagating towards the lens.

The strategy for manufacturing a microlens with a defined focal length and NA is explained with the aid of Fig. 4, where we plot the focal length, optically determined as detailed above and in Fig. 3, as a function of deposition time, for four surfaces irradiated with different doses. The solid curves are a guide to the eye (not a fit) suggesting a plausible trend of the focal length with the deposition time, for the four surfaces measured. The dashed curves are similarly suggested trends for surfaces of different treatments, not measured. each of these curves represents a constant NA, labeled as NA_1–NA_8. Four of the values can be calculated from the (optically) measured focal length and the diameter determined with AFM, using $nD/2f$, with $n=1.5$ (glass). These values are $\text{NA}_1=0.382$, $\text{NA}_2=0.366$, $\text{NA}_6=0.244$, and $\text{NA}_8=0.238$. The NA for the rest of the (dashed) curves can be assumed to take values according to the same rule: NA_i decreases as i increases.

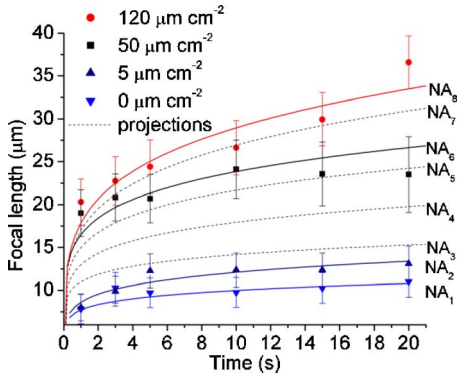

FIG. 4. (Color online) Plot of focal lengths against deposition time for treated surfaces and control. The colored lines are visual aids, illustrating the trend of the focal length to increase with deposition time. The dashed curves indicate the same trend for other possible surface treatments, leading to other NA values. $\text{NA}_1=0.255$, $\text{NA}_2=0.244$, $\text{NA}_6=0.163$, and $\text{NA}_8=0.159$.

The desired NA can be chosen, and the corresponding deposition time may be selected accordingly. A lens of $f=20$ μm can be made with $\text{NA}_8=0.238$ with a ~1.8 s deposition on a surface irradiated with 120 μC cm^{-2}, while a lens of the same focal length but with $\text{NA}_6=0.244$ can be made with a ~3.4 s deposition on a surface irradiated with 50 μC cm^{-2}.

The low electron irradiation wettability tuning method is extremely useful, since it modulates wettability without the introduction of foreign chemical species on the surface. In the context of biochips, this is an important factor, since the additional chemical species may interfere or conflict with surface chemistry required for immobilization, blocking, etc. Problems regarding homogeneity of surface treatment are readily avoided in this approach. Moreover, the method can be readily used to inscribe patterns of various wettabilities on surfaces (by electron irradiation through a mask, or e-beam[8]), thus lenses with various numerical aperture can be easily fabricated on the same substrate, in different regions.

This work has been partially supported by Grant No. 346/00 from the Israel Science Foundation and Grant No. 01-01-01328 from the Israel Ministry of Science, Culture and Sports.

[1]L. M. Demers, D. S. Ginger, S. J. Park, Z. Li, S. W. Chung, and C. A. Mirkin, Science **296**, 1836 (2002).
[2]A. Bruckbauer, D. J. Zhou, L. M. Ying, Y. E. Korchev, C. Abell, and D. Klenerman, J. Am. Chem. Soc. **125**, 9834 (2003).
[3]M. Sokuler and L. A. Gheber, Nano Lett. **6**, 848 (2006).
[4]J. Lahann and R. Langer, MRS Bull. **30**, 185 (2005).
[5]M. Mrksich and G. M. Whitesides, Annu. Rev. Neurosci. **25**, 55 (1996).
[6]G. Rosenman, D. Aronov, and Dekhtyar Yu., U.S. Patent No. 60,730,021 (2005).
[7]D. Aronov, R. Rosen, E. Z. Ron, and G. Rosenman, Process Biochem. (Oxford, U.K.) **41**, 2367 (2006).
[8]D. Aronov, G. Rosenman, A. Karlov, and A. Shashkin, Appl. Phys. Lett. **88**, 163902 (2006).
[9]L. Morbitzer and A. Scharmann, Z. Phys. **181**, 67 (1964).